

# A Solvent-Free Thermosponge Nanoparticle Platform for Efficient Delivery of Labile Proteins

Won Il Choi,<sup>†</sup> Nazila Kamaly,<sup>†</sup> Lorena Riol-Blanco,<sup>‡</sup> In-Hyun Lee,<sup>†</sup> Jun Wu,<sup>†</sup> Archana Swami,<sup>†</sup> Cristian Vilos,<sup>†,§</sup> Basit Yameen,<sup>†</sup> Mikyung Yu,<sup>†</sup> Jinjun Shi,<sup>†</sup> Ira Tabas,<sup>||,⊥,#</sup> Ulrich H. von Andrian,<sup>‡</sup> Sangyong Jon,<sup>▽</sup> and Omid C. Farokhzad<sup>\*,†,○</sup>

<sup>†</sup>Laboratory of Nanomedicine and Biomaterials, Department of Anesthesiology, Brigham and Women's Hospital and <sup>‡</sup>Department of Microbiology and Immunobiology, Division of Immunology, Harvard Medical School, Boston, Massachusetts 02115, United States

<sup>§</sup>Center for Integrative Medicine and Innovative Science, Faculty of Medicine, Universidad Andres Bello, Santiago, Chile

<sup>||</sup>Department of Medicine, <sup>⊥</sup>Department of Pathology and Cell Biology, and <sup>#</sup>Department of Physiology, Columbia University, New York, New York 10032, United States

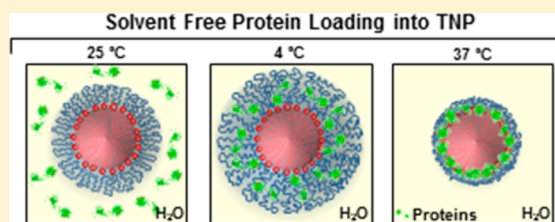
<sup>▽</sup>KAIST Institute of the BioCentury, Department of Biological Sciences, Korea Advanced Institute of Science and Technology (KAIST), Daejeon 305-701, Republic of Korea

<sup>○</sup>King Abdulaziz University, Jeddah 21589, Saudi Arabia

## Supporting Information

**ABSTRACT:** Protein therapeutics have gained attention recently for treatment of a myriad of human diseases due to their high potency and unique mechanisms of action. We present the development of a novel polymeric thermosponge nanoparticle for efficient delivery of labile proteins using a solvent-free polymer thermo-expansion mechanism with clinical potential, capable of effectively delivering a range of therapeutic proteins in a sustained manner with no loss of bioactivity, with improved biological half-lives and efficacy in vivo.

**KEYWORDS:** Nanoparticles, thermosponge, solvent-free, therapeutic proteins, biologics



Since the discovery of insulin in the last century, there has been drive to develop improved methods for the delivery of proteins to patients via pulmonary,<sup>1,2</sup> nasal,<sup>3,4</sup> and oral routes.<sup>5–7</sup> The main avenues of research in the field of biologics delivery involve either the chemical modification of proteins with sugars,<sup>8,9</sup> amino acids,<sup>10</sup> or pegylation,<sup>11,12</sup> or the encapsulation, entrapment, or incorporation of proteins within carriers.<sup>5,13–15</sup> Nanotechnology has played a major role in the design of optimal delivery carriers for biologics with polymeric nanoparticles being particularly effective platforms for protein delivery due to the possibility of fine-tuning their overall biophysicochemical properties<sup>16</sup> in addition to their ability to protect and release proteins in a controlled manner.<sup>17–20</sup> Given that almost a century has passed since the discovery of insulin, the clinical translation of protein drugs and protein-delivering nanomedicines has been a very slow process. This is mainly due to the persistence of major hurdles in the development and manufacturing of protein-based therapeutics that must be overcome to achieve clinical translation. Limitations such as synthetic chemical coupling<sup>21</sup> and formulation parameters such as homogenization, sonication, extrusion, and exposure to solvents lead to the inactivation of biologics;<sup>22–24</sup> thus, discovery of novel methods of formulation and delivery are of importance and highly timely.

Here we show the development of a novel two-stage polymeric thermosponge nanoparticle (TNP) capable of

entrapping a range of proteins in a solvent-free manner, with sustainable bioactivity postrelease (Figure 1). Our TNPs, which incorporate poly(D,L-lactide) (PLA) as the core and Pluronic F127 polymer as the thermosponge shell, are capable of delivering highly potent proteins such as interleukin 10 (IL-10), erythropoietin (EPO), insulin, and human growth hormone (hGH). These were chosen as model proteins because they contain amino acids that produce positive (IL-10 and EPO) or negative (insulin and hGH) electrostatic charges. In addition, these proteins have highly potent therapeutic effects in various diseases including atherosclerosis (IL-10),<sup>25</sup> rheumatoid arthritis (IL-10),<sup>26</sup> anemia (EPO),<sup>27</sup> diabetes (insulin),<sup>5</sup> and Turner's syndrome (hGH).<sup>28</sup> The TNPs significantly improved half-life and systemic exposure of important and potent proteins such as IL-10 and insulin in wild-type mice, as well as the in vivo efficacy of IL-10. These TNPs may offer improved therapeutic effects in vivo compared with native proteins, owing to the integrity of protein bioactivity and long circulation of proteins loaded inside the hydrophilic sponge shell layer. Thus, the developed TNPs have promising potential

**Received:** August 4, 2014

**Revised:** September 19, 2014

**Published:** October 21, 2014

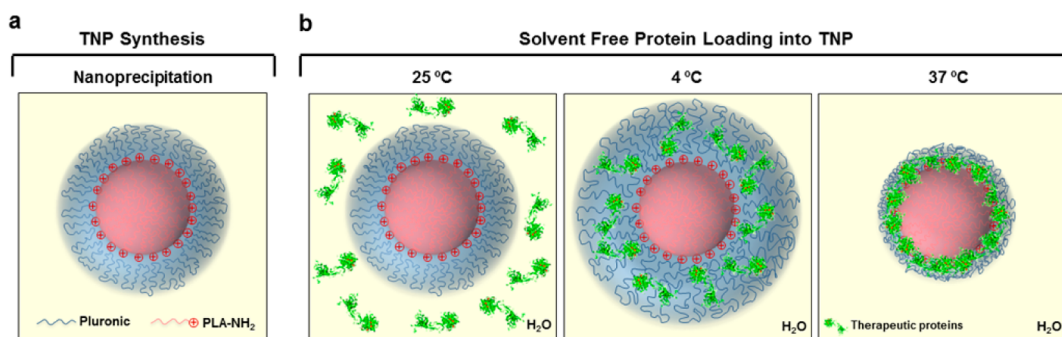


**Figure 1.** Schematic illustration of a thermosponge nanoparticle (TNP) platform. (a) TNP preparation by a one-step nanoprecipitation method. (b) Solvent-free method of protein-loading into TNPs for efficient delivery of labile therapeutic protein drugs. TNPs can be efficiently loaded with desired proteins in a thermoresponsive manner without organic solvents due to the combination of the thermoresponsive swelling behavior of the Pluronic shell of TNPs at 4 °C and the electrostatic interactions between the absorbed proteins and the PLA core of TNPs. The positively charged and negatively charged PLA cores of TNPs were synthesized using PLA-NH<sub>2</sub> and PLA-COOH, respectively, and were tested for loading of relevant therapeutic proteins such as slightly positively charged proteins [IL-10 (isoelectric point (pI) 7.9) EPO (pI 8.3)] and negatively charged proteins [Insulin (pI 5.3) and hGH (pI 5.2)] in deionized water.

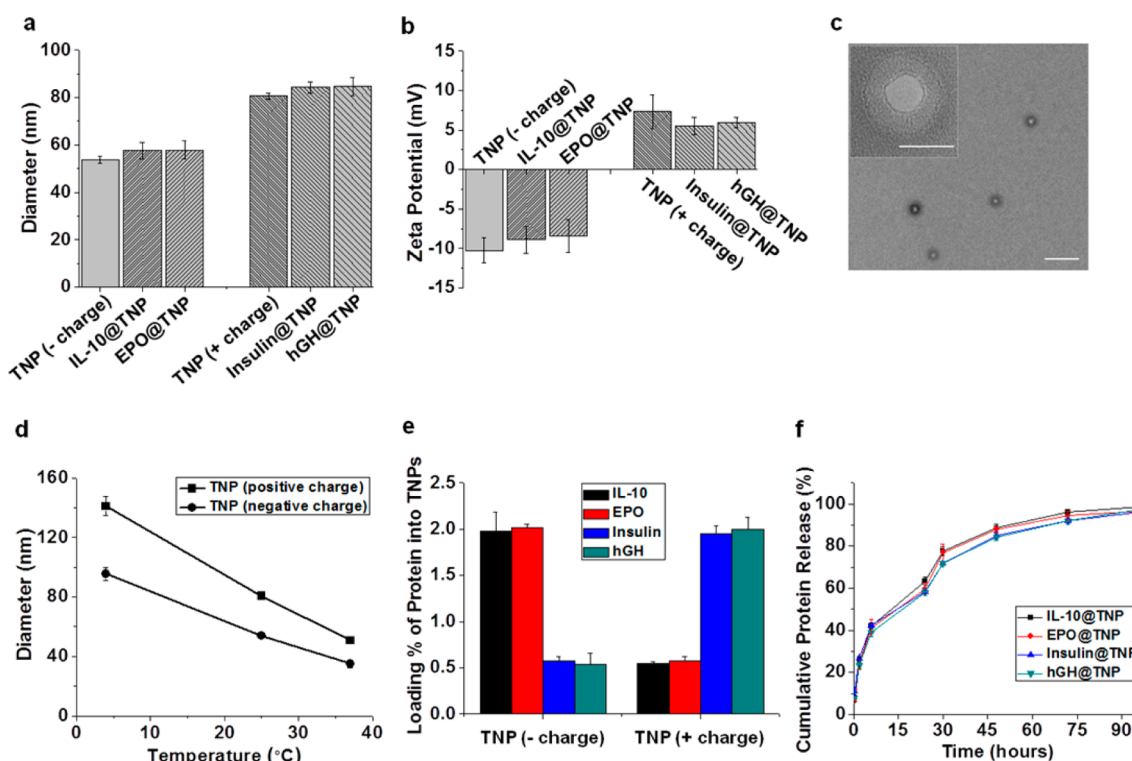


**Figure 2.** Characterization of TNPs. (a) Hydrodynamic diameters and (b) surface charges of TNPs and therapeutic protein-loaded TNPs. (c) Representative TEM image of TNPs. The scale bar is 500 nm. Inset is a high-magnification image with the scale bar representing 50 nm. (d) Swelling and deswelling behavior of TNPs in response to temperature changes. (e) Loading contents (wt %) of therapeutic proteins (IL-10, EPO, insulin, and hGH) into negatively charged or positively charged TNPs. (f) In vitro cumulative release patterns of therapeutic proteins from TNPs in PBS buffer at 100 rpm and 37 °C, analyzed by ELISA (mean  $\pm$  SD,  $n = 3$ ).

for future clinical translation as a solvent-free, scalable, and biocompatible protein-delivery platform.

#### Preparation of Thermosponge Nanoparticle Platform.

We developed a nanoparticle platform composed of biocompatible and biodegradable polymers (PLA, PLGA, and Pluronic) already approved by the FDA (and therefore readily applicable to clinical trials) via a facile single-step nanoprecipitation method. First, the composition ratio of the core and shell layer was optimized for the preparation of TNPs with stability and small size (<100 nm), using PLGA or PLA with carboxy terminals as a core component, and Pluronic F127 as a

shell component. The TNPs were developed in various sizes with core polymer/shell polymer ratios varying from 1:0 to 1:20. Size and zeta potentials ranged from  $151 \pm 4$  nm,  $-31.2 \pm 0.6$  mV (in the case of PLA-based TNPs, 1:0) and  $137 \pm 3$  nm,  $-55.5 \pm 3.2$  mV (in the case of PLGA-based TNPs, 1:0), to  $51 \pm 3$  nm,  $-10.3 \pm 0.9$  mV (in the case of PLA-based TNPs, 1:20) and  $84 \pm 1$  nm,  $-23.5 \pm 3.2$  mV (in the case of PLGA-based TNPs, 1:20) (Supporting Information, Figure S1). Notably, in the case of PLA-based TNPs the NPs were more stable than PLGA-based TNPs in PBS with 10% FBS, as well as in a resuspended state after lyophilization, indicating a

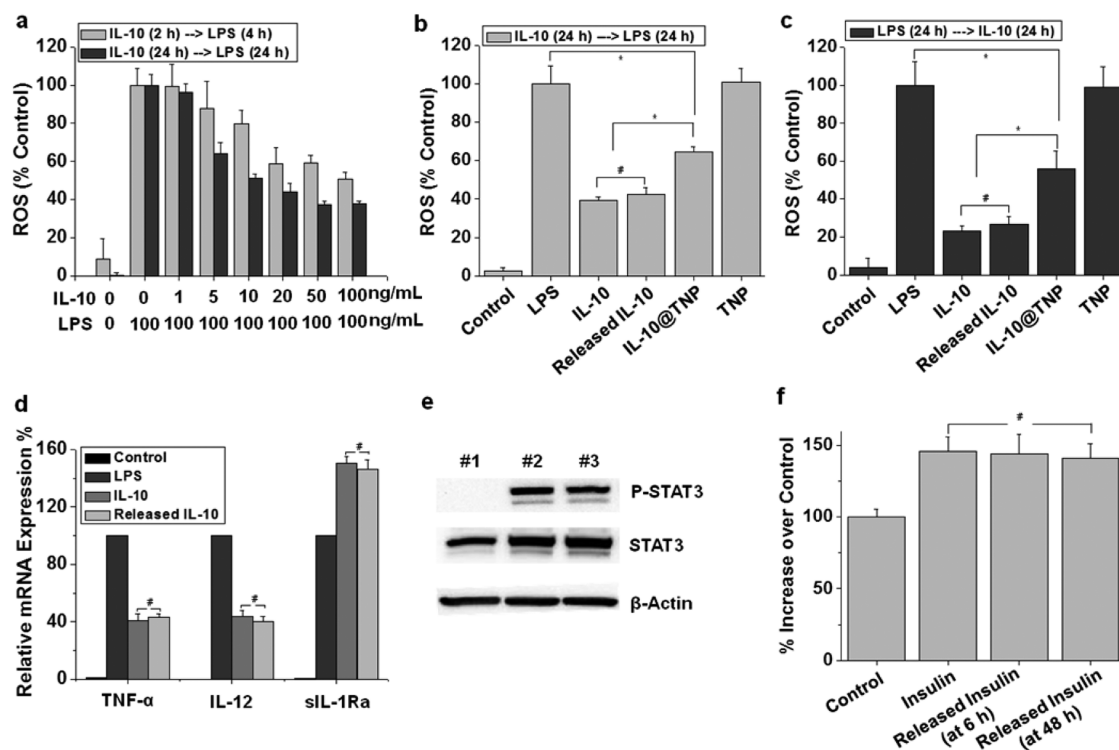


**Figure 3.** Bioactivity of proteins released from TNPs. (a) Inhibitory effects on reactive oxygen species (ROS) production by IL-10 at various concentrations (1–100 ng/mL). Intracellular ROS generated from RAW 264.7 macrophage cells by LPS stimulation was measured using a ROS detection reagent. Bioactivity analysis of the inhibitory effects of native IL-10, released IL-10, and loaded IL-10 on ROS production (b) by pretreatment and (c) by post-treatment of IL-10 ( $n = 3$ , \*  $p < 0.05$ , #  $p > 0.05$ ). (d) Relative mRNA expression of TNF- $\alpha$ , IL-12, and sIL-1Ra after LPS treatment (500 ng/mL) for 4 h, followed by treatment with IL-10 (native IL-10 or released IL-10 at 20 ng/mL) for 2 h at 37 °C ( $n = 3$ , #  $p > 0.05$ ). (e) Western blots were performed to analyze the bioactivity of IL-10 released from TNPs after treatment with IL-10 (native IL-10 or released IL-10 at 20 ng/mL) for 24 h at 37 °C. #1, control; #2, native IL-10; and #3, released IL-10. (f) Bioactivity analysis of native insulin and released insulin (10 nM) on the improved proliferation effect of insulin-dose-dependent human breast cancer cell line MCF-7 ( $n = 3$ , #  $p > 0.05$ ).

stronger hydrophobic interaction between the PLA and Pluronic polymers (Supporting Information, Figure S3). In addition, the NPs showed high encapsulation efficiency (90%) and loading content (4.3 wt %) of lysozyme as a model protein with positive charge and controlled-release kinetics up to a week in PBS as well as PBS (10% FBS), implying that a sufficient amount of protein drug, could be delivered within a reasonably short period to the target site (Supporting Information, Figure S4). In the cytotoxicity test, NPs ranging from 0.1 to 10 mg/mL did not affect the metabolic activity of RAW 264.7 macrophage cells for both 24 and 72 h incubation periods (Supporting Information, Figure S5). Therefore, we determined the optimal formulation to be PLA as a core material, Pluronic F127 as a thermosponge shell, and a core/shell ratio of 1:20 for a nanoparticle platform (with a negative charge or positive charge core) to deliver various therapeutic proteins with positive charges (IL-10, EPO, etc.) or negative charges (Insulin, hGH, etc.).

**Protein-loaded TNPs via a solvent-free encapsulation method.** TNPs (1:20 ratio), optimized for physicochemical characteristics and stability, were prepared by the nanoprecipitation method as described above. In the case of the negatively charged TNPs (PLA-COOH as a core), the hydrodynamic size and surface charge were  $54 \pm 1$  nm and  $-10.2 \pm 1.6$  mV, respectively, whereas the positively charged TNPs (PLA-NH<sub>2</sub> as a core) were  $81 \pm 1$  nm in size and had a surface charge of  $7.3 \pm 2.1$  mV (Figure 2a,b). Interestingly, both TNPs demonstrated similar temperature-responsive

swelling/deswelling Pluronic shell behavior such as change in size  $\sim 96$  nm at 4 °C,  $\sim 54$  nm at 25 °C, and  $\sim 35$  nm at 37 °C (in the case of negatively charged TNPs) and  $\sim 141$  nm at 4 °C,  $\sim 81$  nm at 25 °C, and  $\sim 51$  nm at 37 °C (in the case of positively charged TNPs) (Figure 2d). In addition, the morphological characteristics of TNPs were assessed using transmission electron microscopy (TEM) after negative staining (Figure 2c). TEM images indicated a spherical core-sponge shell structure for the negatively charged NPs, and similar diameters were obtained with dynamic light scattering. The positively and negatively charged TNPs showed very similar results. The core-sponge shell structure is also clearly visible in the high-magnification image in the inset of Figure 2c and easily discriminated when compared with the morphology of PEG-PLA nanoparticles (Supporting Information, Figure S6).

Next, therapeutic proteins (both positively charged IL-10 and EPO and negatively charged insulin and hGH) were successfully loaded into each type of TNP without organic solvents, using two driving forces: (1) the electrostatic interaction between a negatively charged or positively charged PLA core and slightly positively charged or negatively charged proteins in deionized water (Figure 2e) and (2) the volume expansion of the Pluronic shell at low temperature (Figure 2d). After loading the proteins into TNPs, the unencapsulated proteins were separated by ultrafiltration and analyzed for loading content ( $\sim 2.0$  wt %) (Figure 2e) and encapsulation efficiency ( $\sim 90\%$ ). Importantly, the physicochemical param-



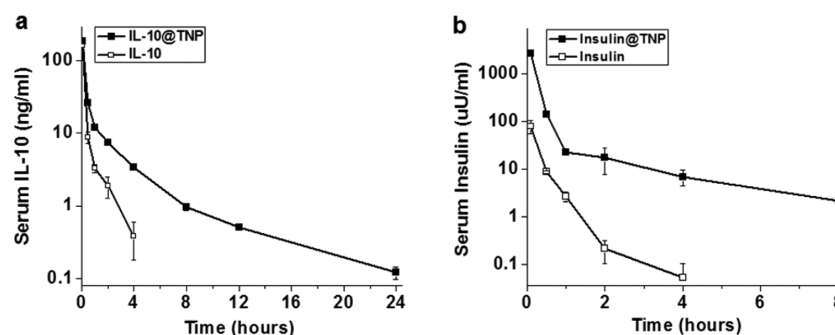


**Figure 4.** Pharmacokinetics of protein-loaded TNPs. Changes in serum protein levels in mice after intravenous administration of (a) IL-10 and IL-10-loaded TNP, and (b) insulin and insulin-loaded TNP. The serum concentrations of proteins were measured at several time points using ELISA kits (mean  $\pm$  SEM,  $n = 3$ ).

ters (size, surface charge, and morphology) of the NPs were not substantially affected by loading the proteins into the NPs (protein@TNP), suggesting that the proteins were effectively shielded (Figure 2a,b). The release profiles of the proteins from the NPs showed similar patterns of sustained release for 4 days without an initial burst because of the swelling with the Pluronic leading to entrapment of the proteins as well as the electrostatic interaction with the PLA core leading to retention of them (Figure 2f). On the basis of these successful results, we further investigated the biological integrity of IL-10 and insulin proteins, as IL-10 has been shown to be a highly potent anti-inflammatory cytokine with potential therapeutic affects in atherosclerosis treatment,<sup>25</sup> and successful insulin delivery is also a highly important unmet medical need.<sup>5</sup>

**Inhibitory Effect of IL-10 on ROS Production.** To analyze the bioactivity of IL-10 released from the NPs, the intracellular reactive oxygen species (ROS) generated from LPS-stimulated RAW 264.7 macrophages was measured with a widely used ROS detection kit (H2DCFDA).<sup>29,30</sup> Before the inhibitory effect of IL-10 on the ROS formation was checked, LPS treatment conditions for cell stimulation were optimized by varying the concentration of LPS (100, 300, and 500 ng/mL) and incubation time (4 and 24 h). Overproduction of ROS increased with stimulation time of LPS with macrophages,<sup>31</sup> whereas the LPS concentration (ranging from 100 to 500 ng/mL) did affect ROS generation but not in a dose-dependent manner, implying that LPS with 100 ng/mL was enough to induce ROS (Supporting Information, Figure S7a). The inhibitory effect of IL-10 on ROS production in LPS-induced macrophages was investigated using various concentrations (1–100 ng/mL) of IL-10 and 100 ng/mL of LPS (Figure 3a). The dose-dependent inhibition effect of IL-10 on ROS production was observed more clearly through the pretreatment of cells with IL-10 for 24 h and stimulation with LPS for 24 h, compared to the shorter induction time of cells pretreated with IL-10 and LPS.<sup>32</sup>

To assess the biological integrity/activity of IL-10 released from NPs, we evaluated native IL-10, IL-10 released from NPs at 48 h, and IL-10-loaded NPs at 50 ng/mL of IL-10 and 100 ng/mL of LPS. In the case of pretreatment of cells with IL-10 (i.e., the prophylactic concept), there was almost no statistical difference between the released IL-10 and native IL-10 ( $p > 0.05$ ) (Figure 3b). Interestingly, in the case of IL-10-loaded NPs, slightly lower activity than the native and released IL-10 indicated that IL-10 was still inside the NPs based on statistical analysis ( $p < 0.05$ ), suggesting both efficient loading and controlled release. More importantly, in the case of post-

treatment of cells with IL-10 (i.e., the therapeutic concept), the inhibitory effect on ROS production was enhanced with all samples; most notably, the bioactivity of released IL-10 was similar to that of the native protein (Figure 3c), indicating that it was maintained during both loading and release.

**Bioactivity Analysis of IL-10 Using qPCR and Western Blot.** To determine whether the IL-10 released from NPs inhibits proinflammatory cytokines produced by inflammatory responses, the relative gene expression levels of TNF- $\alpha$  and IL-12 were compared with the native IL-10 through qPCR (Figure 3d). Expression was dramatically increased after LPS stimulation and the released IL-10 reduced the expression of cytokines (ca. 2.5-fold), suggesting that the released IL-10 not only retains bioactivity, but also functions as an anti-inflammatory cytokine, with results similar to native IL-10. In addition, IL-10 treatment increased sIL-1Ra promoter activity by 1.5-fold compared to LPS alone, and the released IL-10 had effects identical to those of the native protein, consistent with the unique response of IL-10 to the gene expression of the secretory interleukin (IL)-1 receptor antagonist (sIL-1Ra) for which previous studies demonstrate the potential to treat metastatic cancers.<sup>33</sup> The gene expression of several cytokines analyzed in this study suggests that the bioactivity of IL-10 released from the NPs was successfully maintained inside the hydrophilic shell.

Western blots were also employed to determine whether the bioactivity of released IL-10 is well maintained. Because IL-10 has been known to signal via the activation of the signal transducer and activator of transcription 3 (STAT3), which is a key mediator of the inflammatory response of macrophages and other immune cell types,<sup>34</sup> the levels of STAT3 and phosphorylated STAT3 (P-STAT3 at Tyr705) were measured. Compared to the control group, the total levels of STAT3 were slightly increased by IL-10 treatment, using  $\beta$ -Actin as a reference protein (Figure 3e). Moreover, the clear band of P-STAT3 was observed in the native IL-10 group, indicating the activation of STAT3 by IL-10 treatment. The levels of STAT3 and P-STAT3 in the native IL-10 and released IL-10 groups (respectively) were almost identical, suggesting that IL-10 maintained biological integrity throughout the loading process and after release.

**Bioactivity Analysis of Insulin Using MCF-7 Cells.** The bioactivity of insulin released from TNPs was analyzed via insulin-dependent proliferation of MCF-7, as reported previously.<sup>35</sup> It was confirmed that the proliferation of MCF-7 cells was insulin dose-dependent from 1 to 500 nM (Supporting Information, Figure S8). We compared the

enhancement in cell growth (over the control group) produced by native insulin and released insulin (6 and 48 h postrelease) at 10 nM concentration in serum-free medium (Figure 3f). As expected, the released insulin produced almost the same increase in cellular metabolic activity as native insulin (no statistical differences,  $p > 0.05$ ), indicating that the bioactivity of proteins released from TNPs was well maintained. Therefore, based on the results of ROS, qPCR, Western blot, and protein-dependent cell proliferation assay, the newly developed nanoparticle platforms (negatively charged and positively charged TNPs) successfully preserve the bioactivity of loaded proteins.

**Pharmacokinetics of Protein-Loaded TNPs.** Protein-loaded TNPs [IL-10@TNPs (100  $\mu\text{g}$  IL-10/kg) and Insulin@TNPs (1 U Insulin/kg)] were administered intravenously to mice, and blood samples were collected at different time points to analyze the serum concentration of proteins (Figure 4). The mean pharmacokinetic parameters of the proteins were assessed by noncompartmental analysis (Table 1). After intravenous (iv)

**Table 1. Pharmacokinetic Parameters<sup>a</sup>**

a		
parameter	IL-10	IL-10@TNP
dose ( $\mu\text{g}/\text{kg}$ )	100	100
clearance ( $\text{mL}\cdot\text{hr}^{-1}\cdot\text{kg}^{-1}$ )	1979.57	1023.18
Vss ( $\text{mL}/\text{kg}$ )	707.27	2179.42
AUC <sub>0-∞</sub> ( $\text{ng}\cdot\text{hr}/\text{mL}$ )	50.52	97.73
MRT (hr)	0.36	2.13
T <sub>1/2</sub> terminal (hr)	0.25	1.48
b		
parameter	insulin	insulin@TNP
dose (U/kg)	1	1
clearance ( $\text{mL}\cdot\text{hr}^{-1}\cdot\text{kg}^{-1}$ )	38512.48	1242.25
Vss ( $\text{mL}/\text{kg}$ )	10159.47	531.18
AUC <sub>0-∞</sub> ( $\mu\text{U}\cdot\text{hr}/\text{mL}$ )	25.97	804.99
MRT (hr)	0.26	0.43
T <sub>1/2</sub> terminal (hr)	0.18	0.30

<sup>a</sup>Pharmacokinetic parameters of (a) IL-10 and IL-10-loaded TNP and (b) insulin and insulin-loaded TNP administered intravenously to mice. The parameters were analyzed using a noncompartmental model. AUC, area under the concentration–time curve; Vss, volume of distribution at steady state; MRT, mean residence time.

administration of IL-10 alone, the serum IL-10 concentration rapidly decreased until the 8 h point, whereas the concentration was maintained up to 24 h when using TNPs (Figure 4a), increasing the area under the serum concentration–time curve (AUC) 1.9-fold (from 50.52 to 97.73  $\text{ng}\cdot\text{hr}/\text{mL}$ ) (Table 1a). In addition, IL-10-loaded TNPs reduced the clearance 1.9-fold (from 1979.57 to 1023.18  $\text{mL}\cdot\text{hr}^{-1}\cdot\text{kg}^{-1}$ ) and improved the half-life 5.9-fold (from 0.25 to 1.48 h) compared with IL-10 alone. Similar results were obtained when insulin-loaded TNPs were injected into mice (Figure 4b). The insulin-loaded TNPs produced a remarkable increase in systemic exposure (30.9-fold, from 25.97 to 804.99  $\mu\text{U}\cdot\text{hr}/\text{mL}$ ) compared with the insulin-alone group (Table 1b). The group using TNPs also showed significantly reduced clearance (31-fold) and prolonged half-life of insulin (1.6-fold). Our results demonstrate that the TNP platform enhances systemic exposure, reduces clearance, and improves half-life of therapeutic proteins, suggesting that TNPs could become standard tools for efficient delivery of proteins for in vivo biomedical applications.

**In vivo efficacy of protein-loaded TNPs.** In order to determine whether TNPs are an efficient delivery platform for protein drugs in vivo, mice were treated systemically with saline, TNPs, IL-10 (100  $\mu\text{g}/\text{kg}$ ), or IL-10-loaded TNPs (100  $\mu\text{g}$  IL-10/kg). At 2 h postinjection, DNFB was then applied topically to the dorsal and ventral aspects of ear skin, and the ensuing inflammatory response was assessed based on the change in ear swelling and the number of the myeloid cells that infiltrated the ear tissue (Figure 5).

It has been shown that IL-10 is capable of reducing inflammation in DNFB-induced allergic contact dermatitis (ACD).<sup>36</sup> As shown in Figure 5a, although the administration of IL-10 resulted in a reduction of ear swelling compared to the saline-treated control, IL-10-loaded TNPs (IL-10@TNPs) reduced ear swelling much more than IL-10 alone. In addition, mice treated with IL-10@TNPs had less edema and myeloid infiltration than mice injected with IL-10 alone (Figure 5b) and showed greater reduction of neutrophil numbers than the saline group (Figure 5c). The TNPs alone did not elicit any anti-inflammatory effect, indicating that the anti-inflammatory actions of IL-10@TNPs was due to IL-10, not the polymeric composition of the TNPs. Taken together, the findings above suggest that TNPs are a promising nanopatform for protein drug delivery, enhancing both the in vivo half-life and efficacy of protein drugs.

Therapeutic proteins (monoclonal antibodies, growth hormones, cytokines, erythropoietin, insulin, interferons, colony-stimulating factors, blood factors, and so forth) have attracted much attention for their great potential in the treatment of specific target diseases.<sup>37–39</sup> It is widely believed that surface modification or addition of a delivery carrier to native proteins could dramatically improve their biological activity, overcoming such limitations as short half-life (reduced activity), instability (denaturation or aggregation), and immunogenicity.

Many carrier systems have been developed and evaluated in preclinical and clinical trials. In our group, Pridgen et al. developed Fc-targeted PEG–PLA nanoparticles for oral delivery of insulin and demonstrated significant biological activity (prolonged glucose suppression) in mice.<sup>5</sup> Johnson et al. reported that hGH-loaded PLGA formulations maintained hGH serum concentrations for more than a month after a single subcutaneous (sc) injection in rhesus monkeys.<sup>40</sup> The pharmacokinetics of insulin was improved using PEG-conjugated liposomes as a delivery carrier, doubling blood circulation time.<sup>41</sup> Dramatic results were also obtained with recombinant IL-2 incorporated into liposome systems and injected sc into mice, increasing plasma circulation time 8-fold compared to native IL-2.<sup>42</sup> In addition, in an effort to slow the rapid clearance of IL-10 in vivo Hamsell et al. reported the effect of PEGylation of IL-10 on the pharmacokinetics and biodistribution of this protein, which resulted in a 2.7-fold increase in systemic half-life.<sup>43</sup> However, though the PEGylated IL-10 showed prolonged blood circulation in vivo, PEGylation may reduce the bioactivity of IL-10 via lowered binding affinity or structural deformation. While polymeric and liposome formulations have been shown to enhance the pharmacokinetics of native proteins in vivo, reported loading amounts (0.5 wt %) were not very high, and organic solvents were necessary in certain formulations.<sup>5</sup>

Other nanotechnologies employed for protein delivery include polyglutamate-vitamin E nanogels, and other polysaccharide NPs based on chitosan building blocks.<sup>44,45</sup>

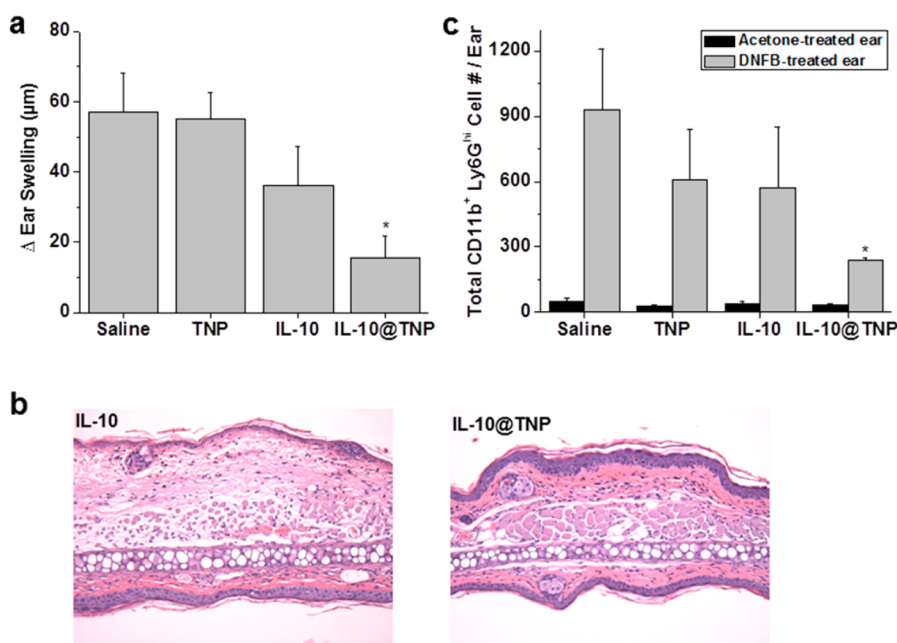


**Figure 5.** In vivo anti-inflammatory efficacy of IL-10-loaded TNPs. (a) Therapeutic efficacy of IL-10 and TNPs on ear swelling in a mouse model of allergic contact dermatitis (ACD) at 100  $\mu$ g IL-10/kg dose via iv administration. (b) Representative histological images of DNFB-treated ears from IL-10 and IL-10-loaded TNP groups. (c) Total neutrophils (CD11b<sup>+</sup>, Ly-6G<sup>high</sup>) in skin at 36 h upon acetone or DNFB challenge. All data are expressed as mean  $\pm$  SEM of  $n = 4$  to 7 per group. \*  $p < 0.05$  for saline vs treatment.

However, the chitosan nanoparticles also showed highly increased size range of 200 to 580 nm as well as noncontrolled initial burst effect of protein drugs.<sup>45</sup> Although these methods also do not use solvents in their preparation, an advantage of the developed TNPs over these previously developed systems in addition to also being solvent-free is that our nanoplatform is applicable to the delivery of a range of proteins with different sizes and charges. Furthermore, the preparation of protein-loaded TNPs is relatively facile and does not require complicated set-ups and relies on simple mixing and electrostatic interactions.

Here we demonstrate a nanoparticle platform with a simple solvent-free encapsulation method. The TNPs showed strong structural stability in a model serum buffer and in resuspension conditions without the need for any cryo-protectants, suggesting that this platform would be amenable to clinical translation. On the basis of the results of ROS, qPCR, Western blot, and protein-dependent cell proliferation assay in vitro, it is clear that the bioactivity of proteins (e.g., IL-10, insulin) was well preserved inside NPs. More importantly, the TNPs significantly increased the half-life and systemic exposure of model therapeutic proteins such as IL-10 ( $t_{1/2}$  5.9-fold) and insulin ( $t_{1/2}$  1.6-fold) in mice without chemical modifications. In addition to increasing the in vivo efficacy of IL-10, these findings highlight the potential of TNPs as a general solvent-free delivery nanoplatform for the efficient delivery of many other therapeutic proteins

## ■ ASSOCIATED CONTENT

### ● Supporting Information

Materials and experimental procedures, notes on TNPs preparations and optimization, stability and release profile, additional TEM images, NMR data, ROS production and optimal LPS concentration, and insulin dose-dependent cell proliferation. This material is available free of charge via the Internet at <http://pubs.acs.org>.

## ■ AUTHOR INFORMATION

### Corresponding Author

\*E-mail: ofarokhzad@zeus.bwh.harvard.edu. Tel: 617-732-6093. Fax: 617-730-2801.

### Author Contributions

W.I.C. and O.C.F. designed the project. W.I.C., N.K., L.R-B., and I.-H.L. performed experiments. W.I.C., N.K., L.R-B., I.-H.L., J.W., A.S., C.V., B.Y., M.Y., J.S., I.T., U.H.v.A., S.J., and O.C.F. contributed to analysis and interpretation of data. W.I.C., N.K., L.R-B., and O.C.F. wrote the paper. All authors discussed and commented on the paper. All authors have given approval to the final version of the manuscript.

### Notes

The authors declare the following competing financial interest(s): O.C.F. has financial interests in BIND Therapeutics, Selecta Biosciences, and Blend Therapeutics, which are developing nanoparticle technologies for medical applications. These companies did not support the aforementioned research and currently have no rights to any technology or intellectual property developed as part of this research..

## ■ ACKNOWLEDGMENTS

This research was supported by the Program of Excellence in Nanotechnology (PEN) Award, Contract #HHSN268201000045C, from the National Heart, Lung, and Blood Institute, National Institutes of Health (NIH), and by NIH Grant CA151884, NIH R01 Grant EB015419-01, and the David Koch-Prostate Cancer Foundation Award in Nanotherapeutics.

## ■ REFERENCES

- (1) Bi, R.; Shao, W.; Wang, Q.; Zhang, N. *J. Biomed. Nanotechnol.* **2009**, *5*, 84–92.
- (2) Smola, M.; Vandamme, T.; Sokolowski, A. *Int. J. Nanomed.* **2008**, *3*, 1–19.



- (3) Kammona, O.; Kiparissides, C. *J. Controlled Release* **2012**, *161*, 781–794.
- (4) Chung, S. W.; Hil-lal, T. A.; Byun, Y. J. *Drug. Target.* **2012**, *20*, 481–501.
- (5) Pridgen, E. M.; Kuo, T. T.; Levy-Nissenbaum, E.; Karnik, R.; Blumberg, R. S.; Langer, R.; Farokhzad, O. C. *Sci. Transl. Med.* **2013**, *5*, 213ra167.
- (6) Bakhru, S. H.; Furtado, S.; Morello, A. P.; Mathiowitz, E. *Adv. Drug Delivery Rev.* **2013**, *65*, 811–821.
- (7) Kamei, N.; Nielsen, E. J.; Khafagy, el-S.; Takeda-Morishita, M. *Ther. Delivery* **2013**, *4*, 315–326.
- (8) Sinclair, A. M.; Elliott, S. J. *Pharm. Sci.* **2005**, *94*, 1626–1635.
- (9) Jain, S.; Hreczuk-Hirst, D. H.; McCormack, B.; Mital, M.; Espenetos, A.; Laing, P.; Gregoriadis, G. *Biochim. Biophys. Acta* **2003**, *1622*, 42–49.
- (10) Baslé, E.; Joubert, N.; Pucheault, M. *Chem. Biol.* **2010**, *17*, 213–227.
- (11) Harris, J. M.; Chess, R. B. *Nat. Rev. Drug Discovery* **2003**, *2*, 214–221.
- (12) Bailon, P.; Berthold, W. *Pharm. Sci. Technol. Today* **1998**, *1*, 352–356.
- (13) Constantinides, P. P.; Wasan, K. M. *Adv. Drug Delivery Rev.* **2004**, *56*, 1239–1240.
- (14) Martins, S.; Sarmiento, B.; Ferreira, D. C.; Souto, E. B. *Int. J. Nanomedicine* **2007**, *2*, 595–607.
- (15) Utama, R. H.; Guo, Y.; Zetterlund, P. B.; Stenzel, M. H. *Chem. Commun.* **2012**, *48*, 11103–11105.
- (16) Kamaly, N.; Xiao, Z.; Valencia, P. M.; Radovic-Moreno, A. F.; Farokhzad, O. C. *Chem. Soc. Rev.* **2012**, *41*, 2971–3010.
- (17) Hasadsri, L.; Kreuter, J.; Hattori, H.; Iwasaki, T.; George, J. M. *J. Biol. Chem.* **2009**, *284*, 6972–6981.
- (18) Moghimi, S. M.; Peer, D.; Langer, R. *ACS Nano* **2011**, *5*, 8454–8458.
- (19) Kobsa, S.; Saltzman, W. M. *Pediatr. Res.* **2008**, *63*, 513–519.
- (20) Yan, M.; Du, J.; Gu, Z.; Liang, M.; Hu, Y.; Zhang, W.; Priceman, S.; Wu, L.; Zhou, Z. H.; Liu, Z.; Segura, T.; Tang, Y.; Lu, Y. *Nat. Nanotechnol.* **2010**, *5*, 48–53.
- (21) Zhang, F.; Liu, M. R.; Wan, H. T. *Biol. Pharm. Bull.* **2014**, *37*, 335–339.
- (22) Pisal, D. S.; Kosloski, M. P.; Balu-Iyer, S. V. *J. Pharm. Sci.* **2010**, *99*, 2557–2575.
- (23) Soppimath, K. S.; Aminabhavi, T. M.; Kulkarni, A. R.; Rudzinski, W. E. *J. Controlled Release* **2001**, *70*, 1–20.
- (24) Choi, W. I.; Tae, G.; Kim, Y. H. *J. Mater. Chem.* **2008**, *18*, 2769–2774.
- (25) Tabas, I.; Glass, C. K. *Science* **2013**, *339*, 166–172.
- (26) Keystone, E.; Wherry, J.; Grint, P. *Rheum. Dis. Clin. North Am.* **1998**, *24*, 629–639.
- (27) Long, D. L.; Doherty, D. H.; Eisenberg, S. P.; Smith, D. J.; Rosendahl, M. S.; Christensen, K. R.; Edward, D. P.; Chlipala, E. A.; Cox, G. N. *Exp. Hematol.* **2006**, *34*, 697–704.
- (28) Choi, W. I.; Kim, M.; Tae, G.; Kim, Y. H. *Biomacromolecules* **2008**, *9*, 1698–1704.
- (29) Chang, L. P.; Lai, Y. S.; Wu, C. J.; Chou, T. C. *J. Pharmacol. Sci.* **2009**, *111*, 147–154.
- (30) Hernández-Ledesma, B.; Hsieh, C. C.; de Lumen, B. O. *Biochem. Biophys. Res. Commun.* **2009**, *390*, 803–808.
- (31) Kim, J. Y.; Choi, W. I.; Kim, Y. H.; Tae, G. *J. Controlled Release* **2011**, *156*, 398–405.
- (32) Dokka, S.; Shi, X.; Leonard, S.; Wang, L.; Castranova, V.; Rojanasakul, Y. *Am. J. Physiol. Lung Cell Mol. Physiol.* **2001**, *280*, L1196–L1202.
- (33) Carl, V. S.; Gautam, J. K.; Comeau, L. D.; Smith, M. F., Jr. *J. Leukocyte Biol.* **2004**, *76*, 735–742.
- (34) Capiralla, H.; Vingtdoux, V.; Venkatesh, J.; Dreses-Werringloer, U.; Zhao, H.; Davies, P.; Marambaud, P. *FEBS J.* **2012**, *279*, 3791–3799.
- (35) Chappell, J.; Leitner, J. W.; Solomon, S.; Golovchenko, I.; Goalstone, M. L.; Draznin, B. J. *Biol. Chem.* **2001**, *276*, 38023–38028.
- (36) Schwarz, A.; Grabbe, S.; Riemann, H.; Aragane, Y.; Simon, M.; Manon, S.; Andrade, S.; Luger, T. A.; Zlotnik, A.; Schwarz, T. J. *Invest. Dermatol.* **1994**, *103*, 211–216.
- (37) Heinemann, L. *Expert. Opin. Biol. Ther.* **2012**, *12*, 1009–1016.
- (38) Orive, G.; Hernández, R. M.; Gascón, R. A.; Domínguez-Gil, A.; Pedraz, J. L. *Curr. Opin. Biotechnol.* **2003**, *14*, 659–664.
- (39) Schmidt, F. R. *Appl. Microbiol. Biotechnol.* **2004**, *65*, 363–372.
- (40) Johnson, O. L.; Cleland, J. L.; Lee, H. J.; Charnis, M.; Duenas, E.; Jaworowicz, W.; Shepard, D.; Shahzamani, A.; Jones, A. J.; Putney, S. D. *Nat. Med.* **1996**, *2*, 795–799.
- (41) Kim, A.; Yun, M. O.; Oh, Y. K.; Ahn, W. S.; Kim, C. K. *Int. J. Pharm.* **1999**, *180*, 75–81.
- (42) Kanaoka, E.; Takahashi, K.; Yoshikawa, T.; Jizomoto, H.; Nishihara, Y.; Hirano, K. *J. Pharm. Pharmacol.* **2001**, *53*, 295–302.
- (43) Alvarez, H. M.; So, O. Y.; Hsieh, S.; Shinsky-Bjorde, N.; Ma, H.; Song, Y.; Pang, Y.; Marian, M.; Escandón, E. *Drug Metab. Dispos.* **2012**, *40*, 360–373.
- (44) Chan, Y. P.; Meyrueix, R.; Kravtsoff, R.; Nicolas, F.; Lundstrom, K. *Expert Opin. Drug Delivery* **2007**, *4*, 441–451.
- (45) Gan, Q.; Wang, T. *Colloids Surf., B* **2007**, *59*, 24–34.